PROCEEDINGS OF SPIE

SPIEDigitalLibrary.org/conference-proceedings-of-spie

# Photonic systems for tunable mm-wave and THz wireless communications

Luis Gonzalez-Guerrero, Katarzyna Balakier, Manoj Thakur, Haymen Shams, Lalitha Ponnampalam, et al.

Luis Gonzalez-Guerrero, Katarzyna Balakier, Manoj Thakur, Haymen Shams, Lalitha Ponnampalam, Chris S. Graham, Martyn J. Fice, Alwyn J. Seeds, Cyril C. Renaud, "Photonic systems for tunable mm-wave and THz wireless communications," Proc. SPIE 10945, Broadband Access Communication Technologies XIII, 109450F (1 February 2019); doi: 10.1117/12.2516041

SPIE.

Event: SPIE OPTO, 2019, San Francisco, California, United States

# Photonic systems for tunable mm-wave and THz wireless communications

Luis Gonzalez-Guerrero[a], Katarzyna Balakier[a], Manoj Thakur[b], Haymen Shams[a], Lalitha Ponnampalam[a], Chris S. Graham[a], Martyn J. Fice[a], Alwyn J. Seeds[a] and Cyril C. Renaud[a]

[a] Department of Electronic and Electrical Engineering, UCL, London WC1E 7JE, U.K
[b] Wivenhoe Park, University of Essex, Colchester CO4 3SQ

## ABSTRACT

In this paper we present two different techniques for photonic generation of millimeter and THz waves. Each of them tackles the phase noise problem associated with optical sources in a different way. The first one relays on the heterodyne down-conversion of two phase noise correlated optical tones. The correlation is achieved by generation of an optical frequency comb. To select one of the optical lines we use an optical phase lock loop, which besides enabling a frequency offset between output and input, can provide optical gain and is highly selective. The second one relays on the envelope detection of a single sideband-with carrier signal. In this approach the photonic remote antenna unit is implemented as monolithically integrated photonic chip.

**Keywords:** Optical phase lock loop, microwave photonics, radio-over-fiber, THz, mm-wave, integrated photonics.

## 1. INTRODUCTION

### 1.1 Photonic generation of millimeter and THz waves for data communication systems

Current projections assume that mm-wave technologies will be needed to meet the long term (i.e. beyond 2020) needs of the mobile communication market. To do this, the network will require the simplification of base stations (BSs) to remote antenna units (RAUs) (i.e. antenna and optoelectronic device) due to the high density of expected BSs (in the order of 100m). In this case, radio over fiber (RoF) tends against the increased cost, as it eliminates the requirement for mm-wave LOs, digital signal processing (DSP) and mixers at the RAU. Moreover, with the utilization of optical fiber infrastructures, new functionalities (i.e. all-optical frequency up-conversion, or optical beamforming) can be utilized in order to further reduce the installation cost, to improve the performance of the wireless services and to expand the use of the current (FTTx-PON) or future (WDM-PON) optical access network. An optimized adaptation/matching of hybrid integrated, energy efficient, wireless, optical and microwave transceiver components, in terms of thermal, electrical & mechanical means is needed to achieve low-cost, energy efficiency and compactness combined with high-bandwidth and improved network coverage. Given the large wavelength offset required between the two optical tones at mm-waves, RoF systems typically used two independent optical sources [1]. This, while ideal in terms of flexibility, makes the generated radio frequency (RF) carrier suffer from frequency fluctuations due to the high phase noise associated with free-running lasers. To compensate this, we present two different types of solutions in this paper.

The first one [2], [3], tackles the problem a priori (i.e., at the transmitter) and relays on the generation of an optical frequency comb. A comb is formed by multiple optical wavelengths all equidistant from each other (comb spacing) and all phase locked to each other. In this technique, two lines of the optical frequency comb spaced at the appropriate frequency separation are filtered individually first. After this, one of them is passed through a modulator driven with a complex signal. Finally, the two tones are optically recombined and sent to the remote antenna unit (RAU). The novelty of the system we present here relays on the filtering scheme we use to select the two comb lines, which is implemented through an optical phase lock loop (OPLL). OPLLs, besides enabling a tunable frequency offset between output and input, provide optical gain, and being highly selective, can be monolithically integrated making them a perfect option for comb filtering. The wireless signal generated in the RAU is recovered in the wireless receiver through optical heterodyne conversion in a mixer. Using this technique, we report a system operating at 250 GHz and 20 Gbit/s. In this proof-of-concept demonstration only one OPLL was available and, thus, only one line could be filtered with this

Broadband Access Communication Technologies XIII, edited by Benjamin B. Dingel, Katsutoshi Tsukamoto, Spiros Mikroulis, Proc. of SPIE Vol. 10945, 109450F
 · doi: 10.1117/12.2516041

technique. In future systems, however, all the comb lines could be selected with this technique, giving unprecedented tuneability capabilities.

In the second one [4], the phase noise is tackled a posteriori (i.e., at the receiver). In this technique an optical tone is modulated with the single sideband (SSB) format and sent to the RAU, where is combined with another laser at the appropriate frequency separation. In the photodiode (PD), a mm-wave SSB signal is generated and sent to the wireless receiver, where an envelope detector (ED) down-converts the signal to intermediate frequency (IF). Since sideband and carrier are coherent to each other, when they beat in the ED the phase noise vanishes from the recovered signal. In the demonstration reported in this paper, the photonic part of the RAU is implemented in the form of a photonic chip where the optical LO, several semiconductor optical amplifiers (SOAs) and a uni-travelling carrier (UTC) PD are monolithically integrated. Using this technique, we report a system operating at 60 GHz and 1 Gbit/s.

In Fig. 1 A and B, we show both techniques fully integrated in a WDM-PON network. As might be expected both techniques have pros and cons. The heterodyne approach (i.e., Fig. 1 A) enables higher sensitivity, which can be exploited to achieve larger transmission distances. The direct detection approach (i.e., Fig 1 B), on the other hand, greatly simplifies the optical transmitter and wireless receiver and may be used where cost is critical.

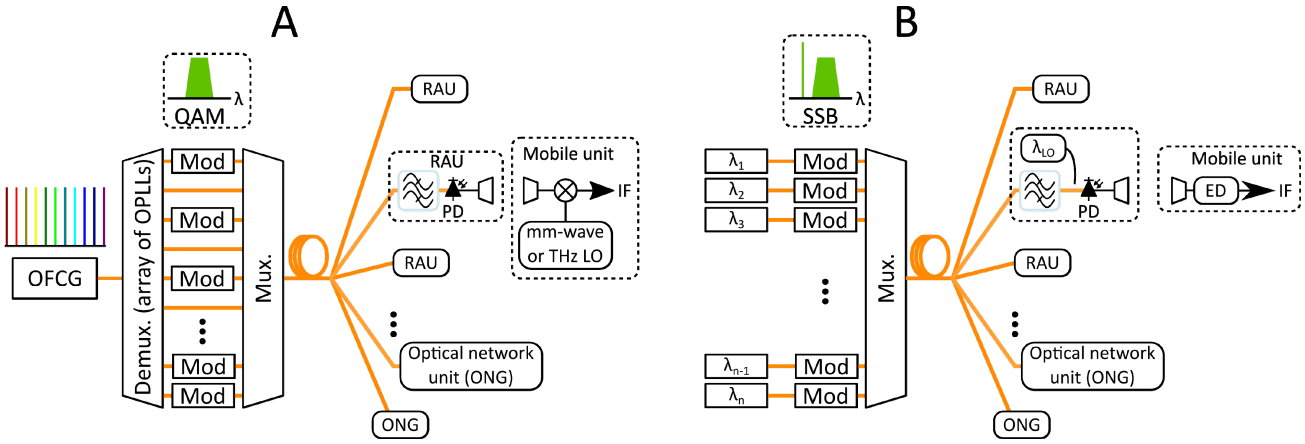


Fig. 1. Schematic representation of a fully converged optical-wireless network using the (A) heterodyne approach with optical frequency comb selection through OPLL and (B) the direct detection approach with free-running lasers.

## 2. HETERODYNE APPROACH

### 2.1 THz Transmission experimental arrangement

The experimental arrangement for the optical tunable coherent THz frequency system using the OPLL is shown in Fig. 2. In the central office (CO), a single wavelength laser source oscillating at 1533.14 nm and with a 10 kHz linewidth is used to generate the optical comb by feeding it to a dual-drive Mach-Zehnder modulator (MZM) [5]. The comb spacing in this case is adjusted to be 15 GHz. The comb output is then optically amplified and split into two optical paths using a 3-dB coupler. One optical tone is selected with a free-space passive filter with a 10 GHz bandwidth, and used for optical data modulation with an IQ optical modulator, which is driven with a 10 Gbaud QPSK signal with square root raised cosine (RRC) filtering and a 0.1 roll-off factor. This electrical signal is generated with an arbitrary waveform generator (AWG) operating at 50 Gsamples/s and passed through two electrical amplifiers before being fed to the IQ modulator. In the lower optical branch, the optical comb is sent to the OPLL sub-system for single line selection and amplification.

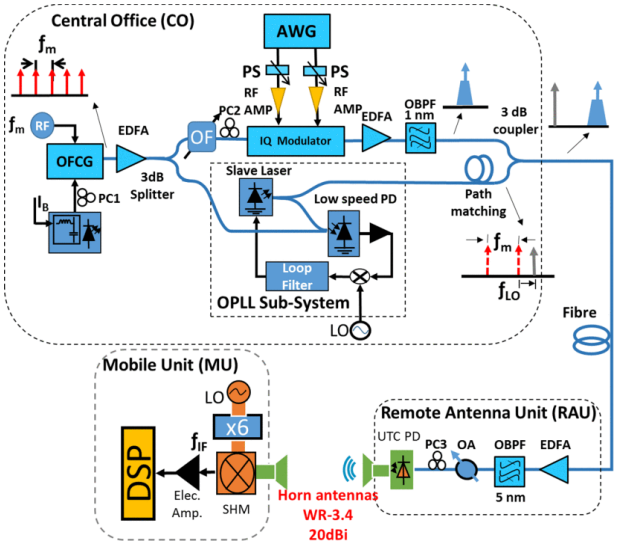


Fig. 2. Experimental arrangement diagram for THz frequency tuneability using OPLL. OFCG: optical frequency comb generator; EDFA: Erbium doped fiber amplifier; PS: phase shifter; PC: polarization controller; OBPF: optical bandpass filter; AWG: arbitrary waveform generator; OPLL: optical phase lock loop; OA: optical attenuator; UTC: uni-travelling carrier; PD: photodiode; SHM: second harmonic mixer; DSP: digital signal processing.

To account for the optical path mismatch between the two arms, compensating fiber is added to the optical branch with the OPLL. After comb filtering and modulation, the output of both optical paths is recombined and sent to the RAU. The received optical signal at this unit is amplified by an erbium-doped fiber amplifier (EDFA) and filtered with a 5 nm optical bandpass filter (OBPF) before being photomixed in a UTC-PD. Horn antennas with 20 dBi gain are used at the THz transmitter and receiver to increase the collimation of the THz beam. The received THz signal at the mobile unit (MU) is down-converted to an intermediate frequency (IF) using a sub-harmonic mixer (SHM). The local oscillator (LO) feeding the SHM is generated with a 6$^{th}$ harmonic multiplier fed by an RF source oscillating at a frequency of 12 GHz.

The down-converted signal is then electrically amplified and captured by a real time scope (RTS) with a 36 GHz bandwidth and a sampling rate of 80 Gsamples/sec. The signal was recorded over a period 10 $\mu$sec which corresponds to 200,000 bits. The received signal is then processed offline with a typical coherent routine including: digital down-conversion, down-sampling (2 Samples/symbol), channel equalization based on a blind equalizer algorithm, frequency offset estimation, and the Viterbi-Viterbi algorithm for phase noise estimation. The bit error rate (BER) is finally calculated after symbol to bit de-mapping. A complete BER curve is obtained by varying the injected optical power into the broad bandwidth PD.

### 2.2 Optical phase lock loop (OPPL)

The OPLL, shown in Fig. 3, consists of a photonic chip and an electronic feedback loop. The photonic integrated chip (PIC) includes a distributed Bragg reflector (DBR) laser, serving as the slave laser, SOA, and a PIN PD [6]. All optoelectronic components are monolithically integrated on a single InP-based chip with dimensions of 2mm × 6mm [7]. The electronic feedback loop (consisting of a bias tee, amplifier, phase detector and bias circuit) controlling the frequency and phase locking of the slave laser was designed using commercially available electronic components.

Inside the OPLL chip the optical comb line gets mixed with the slave laser on the integrated PD. In order to select a specific comb line with the OPLL, the wavelength of the DBR laser is set close to the chosen line by adjusting the laser grating currents. The output heterodyne signal is then amplified, and its phase compared with an RF reference. This generates a feedback signal that is used to adjust the phase of the slave laser. It should be noted that the frequency offset between the comb line and the slave laser is precisely specified by the frequency of the RF reference, and therefore can be tuned with the same precision as the RF synthesizer. In this particular OPLL, the offset frequency tuning ranges between 4 and 12 GHz. However, OPLLs with higher offset frequency have been reported in literature [8].

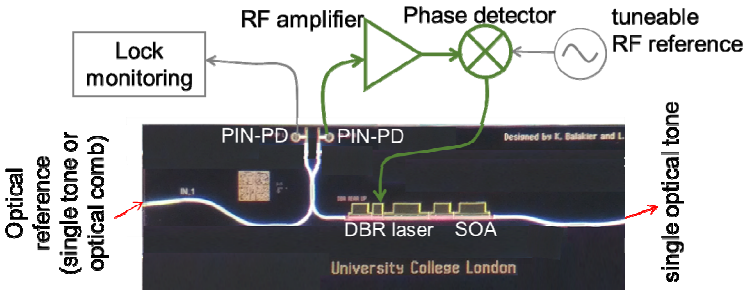


Fig. 3. OPLL PIC with schematic representation of the electronic loop.

### 2.3 OPLL results

Fig. 4(a) shows the optical spectra of the optical comb and the OPLL output. As can be seen, all the unwanted optical comb lines are suppressed by more than 50 dB in the OPLL (measured with 10 MHz resolution bandwidth). One can also see how the OPLL output can be precisely offset from the selected comb line. It is important to mention that the wavelength of the slave laser can be positioned on the lower or the upper side of the selected comb line.

In Fig. 4(b), the RF reference is adjusted to give offset frequencies of 4.2 GHz and 6 GHz from an optical comb line which is separated by 15 comb lines (225 GHz) from the comb line used for data modulation. This gives THz carriers at 229.2 GHz and 231 GHz, respectively. To tune to higher THz carrier frequency, the wavelength of the slave laser is set to be close to the optical comb line spaced by 16 optical lines (240 GHz). This generates THz frequencies of 235.9 GHz, and 244 GHz by setting the OPLL RF reference frequency at 4.1 GHz, and 4.0 GHz, respectively.

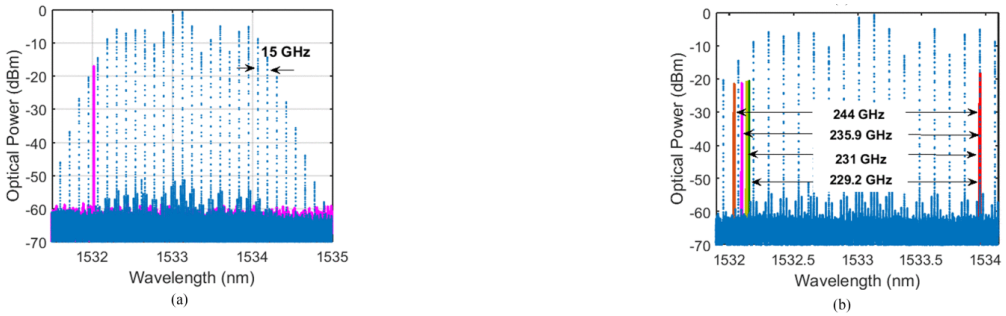


Fig. 4. Optical spectra of (a) the OFCG (dotted blue lines), and the OPLL sub-system output (solid pink line), and (b) the OFCG (dotted blue lines), and the optical lines generated from the OPLL when the OPLL is locked at different offset frequencies; 4.2 GHz (green line), and 6 GHz (yellow line) spaced by 15 comb line from the selected comb line (red line) at the upper arm, and at 4.1 GHz (pink line) and 4 GHz (brown line) spaced by 16 comb lines.

When no data was being sent (i.e., none of the lines was modulated), the spectrum of the down-converted THz signal at the MU was measured with an electrical spectrum analyzer (ESA) to see the OPLL stabilization effect on the DBR laser. Fig. 5(a) shows the obtained spectra in the ESA with a max hold function set to 20 seconds when the OPLL is locked and unlocked, at a frequency of 229.5 GHz. When the OPLL is inactive, the slave laser is in a free-running mode, and the frequency of the generated THz carrier fluctuates within a range of ~200 MHz. This is due to the thermal instabilities of the two free running lasers, and would require a frequency tracking technique in the receiver. However, when the OPLL is locked, the THz frequency is fixed exhibiting an increase in the carrier peak power. The sideband peaks around the carrier (at the offset frequency of ±80 MHz) result from the loop bandwidth limitation. When the OPLL is active, the phase noise of the generated carrier is suppressed within the loop bandwidth [9].

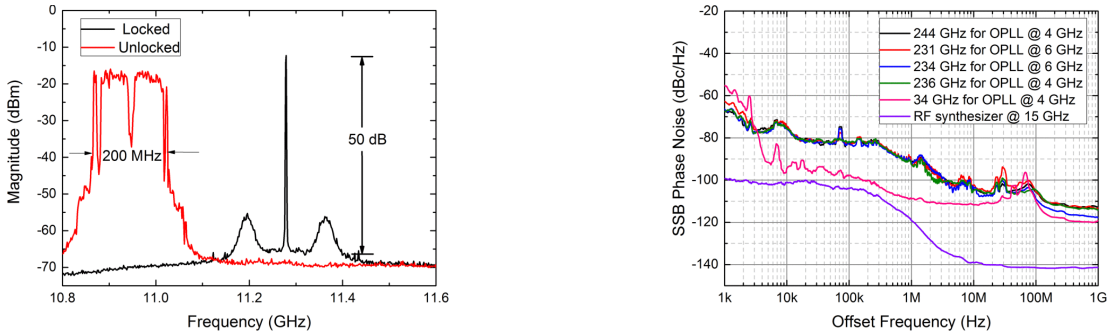


(a) (b)

Fig. 5. (a) Phase noise measurements of the heterodyne mixing between OPLL output and optical carrier spaced at 34 GHz, 231 GHz, 234 GHz, 236 GHz, 244 GHz, and RF synthesizer used in the OFCG and (b) electrical spectra of the THz carrier down-converted to IF frequency when the OPLL is active and inactive. The resolution, and video bandwidth of the spectrum analyzer were set to 300 kHz, and 100 kHz, respectively.

Furthermore, the phase noise of the heterodyne mixing between the OPLL output and an optical comb line spaced at 34 GHz, 231 GHz, 234 GHz, 236 GHz, and 244 GHz were measured using a Rohde&Schwarz FSU43 ESA, and compared with the phase noise of the RF synthesizer (operating at 15 GHz) used to generate the comb lines, as shown in Fig. 5(b) The phase noise measurements for frequencies at 231 GHz, 234 GHz, 236 GHz, and 244 GHz show a residual phase noise level of less than −85 dBc/Hz at 10 kHz offset from carrier, when the OPLL is active and locked at 4 GHz and 6 GHz offsets from the selected comb line. This is approximately 15 dB higher than the phase noise measurements at 34 GHz, as expected due to frequency multiplication [10]. We can also see the sideband peaks at about 80 MHz resulting from the OPLL bandwidth. The spurious peaks at 70 kHz, and 30 MHz seem to be coupled from laboratory environment through the unpackaged OPLL.

### 2.4 THz Transmission results

Fig. 6 shows the BER measurements versus the received electrical power for four THz signals at carrier frequencies of 229.2 GHz, 231 GHz, and 235.9 GHz. There are only small differences between the BER curves, and all the results are below the hard decision forward error correction (HD-FEC) limit of $3.8 \times 10^{-3}$ (7% overhead bits).

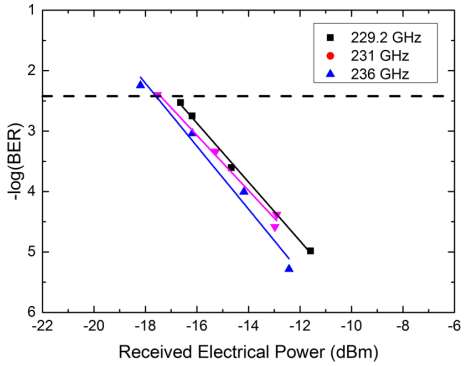


Fig. 6. BER measurements versus electrical received power where the THz carrier is tuned for three different frequencies.

## 3. DIRECT DETECTION APPROACH

### 3.1 Millimeter wave Transmission arrangement

The experimental assembly used in the wireless transmission of the 60 GHz carrier signal [6] is shown in Fig. 7. The SSB-with carrier (SSB-WC) signal was generated by modulating a distributed feedback (DFB) laser (oscillating at 1559.4 nm) with an Orthogonal Frequency Division Multiplex (OFDM) waveform in an external dual drive Mach-Zehnder modulator (DD-MZM). The SSB-WC signal was optically transmitted from the CS to the photonic integrated RAU through 100 m of optical fiber. The incoming signal was then coupled into the optical waveguide on the PIC and

subsequently photomixed with the optical LO on the integrated UTC-PD. The optical LO was lasing at 1558.8 nm, which corresponds to a frequency offset of 60 GHz whit respect to the DFB laser at the CS. The two optical signals were continuously monitored on the optical spectra analyser (OSA) as presented in Fig. 8 (a).

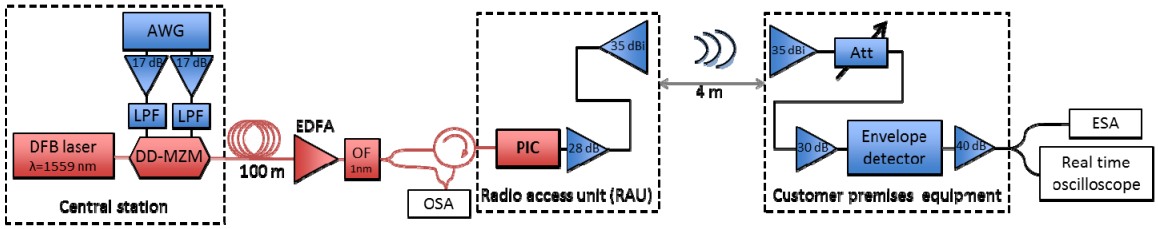


Fig. 7. Schematic of the experimental assembly of the 60 GHz wireless transmission link consisting of central station unit where OFDM data is modulated on single optical tone, a wireless transmitter based on monolithically integrated LO and optical-to-electrical converter, a wireless signal detection unit and monitoring equipment such as spectrum analyzers.

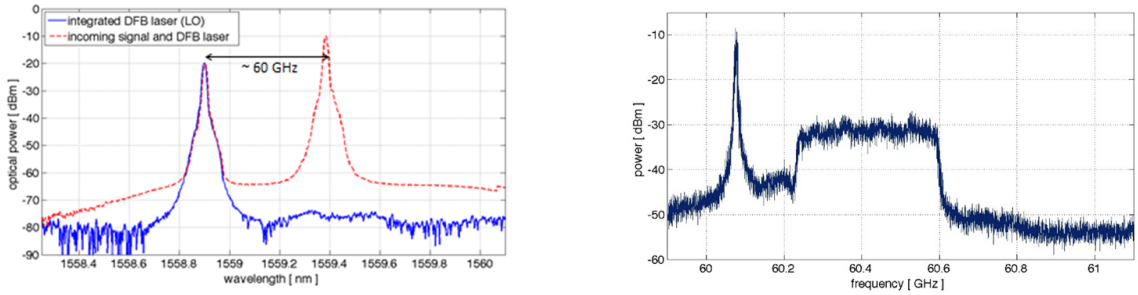


(a) (b)

Fig. 8. (a) Optical spectra of the 60 GHz spaced signals. The incoming signal from central office (in red) and the DFB laser (optical LO) integrated on the chip (in blue) and (b) Electrical spectrum of the 60 GHz carrier and OFDM data measured at the input to the envelope detector (RBW= 1MHz, VBW=50kHz).

The millimetre-wave signal generated at the output of the UTC-PD was coupled with a coplanar waveguide line, which was accessed through a ground-signal-ground high frequency probe. The generated millimetre-wave signal was first amplified by a high power amplifier with 28 dB gain and then transmitted wirelessly using Cassegrain antennas with 35 dBi gain.

The receiving antenna was located at 4 m distance from the transmitter and was used to capture the OFDM signal at 60 GHz. Once detected, the received signal was amplified using a broadband (50-67 GHz) low noise amplifier with 30 dB gain. After the amplifier, the signal was down-converted using an envelope detector based on a zero-biased Shottky diode design to operate within the V-band (50-75 GHz). The signal at an IF frequency of around 350 MHz was once more amplified and split to be observed on an electrical spectrum analyser and real time oscilloscope. Finally, the data set was acquired on a 50 GS/s sampling rate oscilloscope and further processed offline in MATLAB. The electrical spectrum of the SSB-WC signal at 60 GHz is presented in Fig. 8 (b), where it can be observed the 380 MHz bandwidth of the OFDM sideband. It should be mentioned that a 350 MHz offset was introduced between the 60 GHz carrier and the centre of the data envelope in order to mitigate the effect of the subcarrier-signal beat interference.

It is expected that the transmission distance could be increased to 23 m, while maintaining high quality wireless transmission. This could be done by removing a variable value attenuator, set to provide at least 15 dB attenuation. The attenuator was implemented following the antenna to prevent the receiving amplifier from reaching the saturation point.

### 3.2 Experimental results

For the OFDM signal a 16-QAM modulation format with 256 subcarriers and 380 MHz bandwidth was used, allowing for a spectral efficiency of 3 bits/s/Hz [6]. Although for this work a single band of OFDM signal was used, the 7 GHz modulation bandwidth capability of the system, only limited by the V-band components, can accommodate 15 such

bands resulting in data rates higher than 10 Gbps. The use of multiple bands can also allow future flexibility in bandwidth allocation to end-users depending on the network topology.

To evaluate the performance of the wireless transmission, link the received signal has been plotted as a constellation diagram presented in Fig. 9, showing that each symbol can be clearly distinguished. The received wireless 16-QAM-OFDM was characterized to have a SNR better than 20 dB and the average frame EVM RMS was -21.43 dB. This corresponded to the received signal BER of $1.27 \cdot 10^{-4}$.

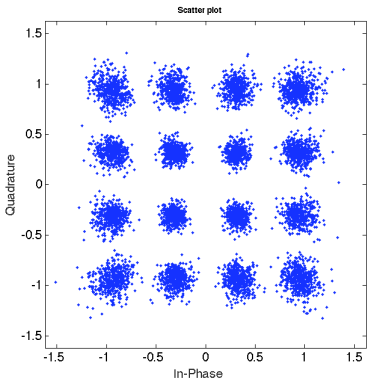


Fig. 9. 16-QAM-OFDM constellation obtained after 100 m on fibre and 4 m wireless transmission.

## 4. CONCLUSIONS

In this paper we demonstrate two different approached realize the mm-wave and THz wireless link. The coherent photonic THz system using an OPLL to select one of the comb lines has been chosen due to the ability of the OPLL to offset its output frequency with respect to the reference comb tone. |This technique offers a perfect solution for those systems where tuning the spacing of the optical frequency comb is not allowed. The OPLL we showed in this paper is implemented in a monolithically PIC which, compared to free-space filters, is ideal for systems where compactness is required. Using this PIC for comb filtering we show a THz system transmitting 10 GBd QPSK signals and operating at various carrier frequencies centered around 232 GHz. The second approach has demonstrated 60 GHz 1.2 Gb/s wireless transmission over 4 m air link that can be increased to over 23 m of transmission distance by simply removing 15 dB attenuation which was introduced to the system. The successful realization of this transmission link demonstrates the potential of the photonic integrated circuits to be implemented in RAU used in 16-QAM- OFDM downlink stream.

## ACKNOWLEDGMENTS

This work was supported in part by the U.K. Engineering and Physical Sciences Research Council (EPSRC) under the Coherent TeraHertz Systems Programme Grant EP/J017671/1, in part by COALESCE (EP/P003990/1), and in part by the EPSRC UKRI Fellowship Grant EP/S000976/1. This project has also received funding from the European Union's Horizon 2020 research and innovation programme under grant agreement 761579 (TERAPOD).

## REFERENCES

[1] A. J. Seeds, H. Shams, M. J. Fice, and C. C. Renaud, "TeraHertz photonics for wireless communications," *J. Light. Technol.*, vol. 33, no. 3, pp. 579–587, 2015.

[2] H. Shams, K. Balakier, M. J. Fice, L. Ponnampalam, C. S. Graham, C. C. Renaud, A. J. Seeds, and F. Van Dijk, "Coherent frequency tuneable thz wireless signal generation using an optical phase lock loop system," *MWP 2017 - 2017 Int. Top. Meet. Microw. Photonics*, vol. 2017–December, pp. 1–4, 2017.

[3] H. Shams, K. Balakier, L. Gonzalez-Guerrero, M. J. Fice, L. Ponnampalam, C. Graham, C. C. Renaud, and A. J. Seeds, "Optical frequency tuning for coherent THz wireless signals," *J. Light. Technol.*, vol. 36, no. 19, pp. 4664–4670, 2018.

[4] K. Balakier, M. P. Thakur, F. Van Dijk, M. Lamponi, M. Chtioui, Y. Leiba, J. E. Mitchell, A. J. Seeds, and C. C. Renaud, "Demonstration of photonic integrated Rau for millimetre-wave gigabit wireless transmission," in *IEEE Topical Meeting on Microwave Photonics (MWP)*, 2016, vol. 6, pp. 344–347.

[5] T. Sakamoto, T. Kawanishi, and M. Izutsu, "Widely wavelength-tunable ultra-flat frequency comb generation using conventional dual-drive Mach-Zehnder modulator," *Electron. Lett.*, vol. 43, no. 19, 2007.

[6] K. Balakier, L. Ponnampalam, M. J. Fice, C. C. Renaud, and A. J. Seeds, "Integrated Semiconductor Laser Optical Phase Lock Loops," *IEEE J. Sel. Top. Quantum Electron.*, vol. 24, no. 1, 2018.

[7] K. Bałakier, M. J. Fice, L. Ponnampalam, C. S. Graham, A. Wonfor, A. J. Seeds, and C. C. Renaud, "Foundry fabricated photonic integrated circuit optical phase lock loop," *Opt. Express*, vol. 25, no. 15, p. 16888, 2017.

[8] U. Gliese, T. N. Nielsen, M. Bruun, E. L. Christensen, K. E. Stubkjaer, S. Lindgren, and B. Broberg, "A Wideband heterodyne optical phase-locked loop for generation of 3–18 GHz microwave carriers," *IEEE Photonics Technol. Lett.*, vol. 4, no. 8, pp. 936–938, 1992.

[9] K. Balakier, H. Shams, M. J. Fice, L. Ponnampalam, C. S. Graham, C. C. Renaud, and A. J. Seeds, "Optical phase lock loop as high-Q filter for optical frequency comb line selection," in *IEEE Topical Meeting on Microwave Photonics (MWP)*, 2017, vol. submited, pp. 1–5.

[10] F. L. WALLS and A. DeMARCHI, "RF spectrum of a signal after frequency multiplication," *IEEE Trans. Instrum. Meas.*, vol. IM, no. 3, pp. 78–80, 1975.